OPTOGENETICS

The rhodopsin–guanylyl cyclase of the aquatic fungus *Blastocladiella emersonii* enables fast optical control of cGMP signaling

Ulrike Scheib,[1]* Katja Stehfest,[1]* Christine E. Gee,[2]* Heinz G. Körschen,[3] Roman Fudim,[1] Thomas G. Oertner,[2]† Peter Hegemann[1]†

Blastocladiomycota fungi form motile zoospores that are guided by sensory photoreceptors to areas of optimal light conditions. We showed that the microbial rhodopsin of *Blastocladiella emersonii* is a rhodopsin–guanylyl cyclase (RhGC), a member of a previously uncharacterized rhodopsin class of light-activated enzymes that generate the second messenger cyclic guanosine monophosphate (cGMP). Upon application of a short light flash, recombinant RhGC converted within 8 ms into a signaling state with blue-shifted absorption from which the dark state recovered within 100 ms. When expressed in *Xenopus* oocytes, Chinese hamster ovary cells, or mammalian neurons, RhGC generated cGMP in response to green light in a light dose–dependent manner on a subsecond time scale. Thus, we propose RhGC as a versatile tool for the optogenetic analysis of cGMP-dependent signaling processes in cell biology and the neurosciences.

INTRODUCTION

Nature has produced very few classes of principal sensory photoreceptors, namely, the rhodopsins, flavoproteins, and phytochromes, which are used by living organisms to orient themselves in an illuminated world. Rhodopsins are used for photosensing whenever speed is required. Until now, three classes of rhodopsins have been identified: the sensory rhodopsins, which activate heterotrimeric guanine nucleotide–binding proteins (G proteins) or histidine kinases; the light-activated ion channels (channelrhodopsins); and the light-driven ion pumps (*1*). Spores of fungi in the family *Blastocladiaceae* are phototactic, requiring cyclic guanosine monophosphate (cGMP) and retinal for photo-orientation, and showing action spectra for photo-orientation that are rhodopsin-like (*2*–*4*). An action spectrum is the plot of the strength of a biological response against the wavelength of the actinic light. A microbial rhodopsin sequence (type I rhodopsin) was identified in the genome of *Blastocladiella emersonii* (*4*). The authors of that study showed that this protein is expressed in the eyespot of the *Blastocladiella* zoospore, and phototactic experiments provided evidence that this rhodopsin functions as a phototaxis photoreceptor (*4*). Furthermore, sequence analysis revealed that the *Blastocladiella* rhodopsin is directly connected to a putative guanylyl cyclase (GC) domain through a 46–amino acid residue linker (Fig. 1A). Interestingly, this molecule has no kinase homology domain, which in other membrane-bound GCs connects the cyclase domain to their transmembrane helices (*5*).

Because such rhodopsin-enzyme hybrids have not been reported before, we characterized the newly discovered rhodopsin-GC (RhGC) spectroscopically and electrophysiologically in heterologous expression systems. Finally, we coexpressed RhGC together with the cGMP-specific cyclic nucleotide–gated A2-channel (CNG-A2) in Chinese hamster ovary (CHO) cells and in rat hippocampal neurons, and confirmed the suitability of RhGC as a previously uncharacterized optogenetic tool to control intracellular cGMP abundance.

[1]Institute for Biology, Experimental Biophysics, Humboldt-Universität zu Berlin, D-10115 Berlin, Germany. [2]Institute for Synaptic Physiology, Center for Molecular Neurobiology Hamburg, University Medical Center Hamburg-Eppendorf, D-20251 Hamburg, Germany. [3]Department of Molecular Sensory Systems, Center of Advanced European Studies and Research (caesar), Ludwig-Erhard-Allee 2, 53175 Bonn, Germany.
*These authors contributed equally to this work.
†Corresponding author. E-mail: hegemann@rz.hu-berlin.de (P.H.); thomas.oertner@zmnh.uni-hamburg.de (T.G.O.)

RESULTS

Characterization of RhGC in *Xenopus* oocytes

We hypothesized that heterologous expression of RhGC would be sufficient to enable optical control of cGMP abundance in cells. To test this, we expressed codon-humanized, RhGC-encoding complementary RNA (cRNA) together with cRNA encoding the cGMP-selective CNG-A2 from rat olfactory neurons ($K_{1/2}^{cAMP} = 36\ \mu M$, $K_{1/2}^{cGMP} = 1.3\ \mu M$) (*6*) in *Xenopus laevis* oocytes. The oocytes were supplemented with all-trans-retinal, which served as the rhodopsin chromophore, and 3 days after cRNA injection, photocurrents were analyzed. Because in previous phototaxis measurements the highest light sensitivity was achieved with green light (*4*), the cells were illuminated for 2 s with 560-nm light. Inward currents gradually increased with light intensity (Fig. 1B), and current slopes saturated with an EC_{50} of 0.028 mW mm^{-2} (Fig. 1C). Varying the duration of the light pulse (0.1 to 1.6 s of 530-nm light) produced photocurrents that were of graded amplitude but nearly constant slope (Fig. 1, D and E). When light was switched on, photocurrents began to increase linearly after 390 ± 35 ms, and the currents continued to increase with no signs of saturation for as long as 30 s at the light intensities used (Fig. 1F). After the light was switched off, the time to the photocurrent peak was 1.9 ± 0.072 s (Fig. 1D).

We tested the specificity of the cyclase by coexpressing RhGC with the CNG-A2 channel mutant C460W/E583M, which is more sensitive to cAMP than to cGMP ($K_{1/2}^{cAMP} = 0.89\ \mu M$, $K_{1/2}^{cGMP} = 6.2\ \mu M$) (*6*). Photocurrents were less than 1% of those observed in experiments with the cGMP-gated CNG-A2 channel, which suggested that RhGC was highly selective for guanosine triphosphate (GTP) (Fig. 1G). In addition, the lack of photocurrents in the absence of the cGMP-sensitive channel suggests that RhGC did not have any substantial intrinsic ion channel or ion-pumping activity. In control experiments with oocytes coexpressing the cAMP-sensitive channel together with the bPAC (*7*), blue light of 450 nm evoked long-lasting photocurrents (Fig. 1G), confirming the functionality of the cAMP-sensitive channel.

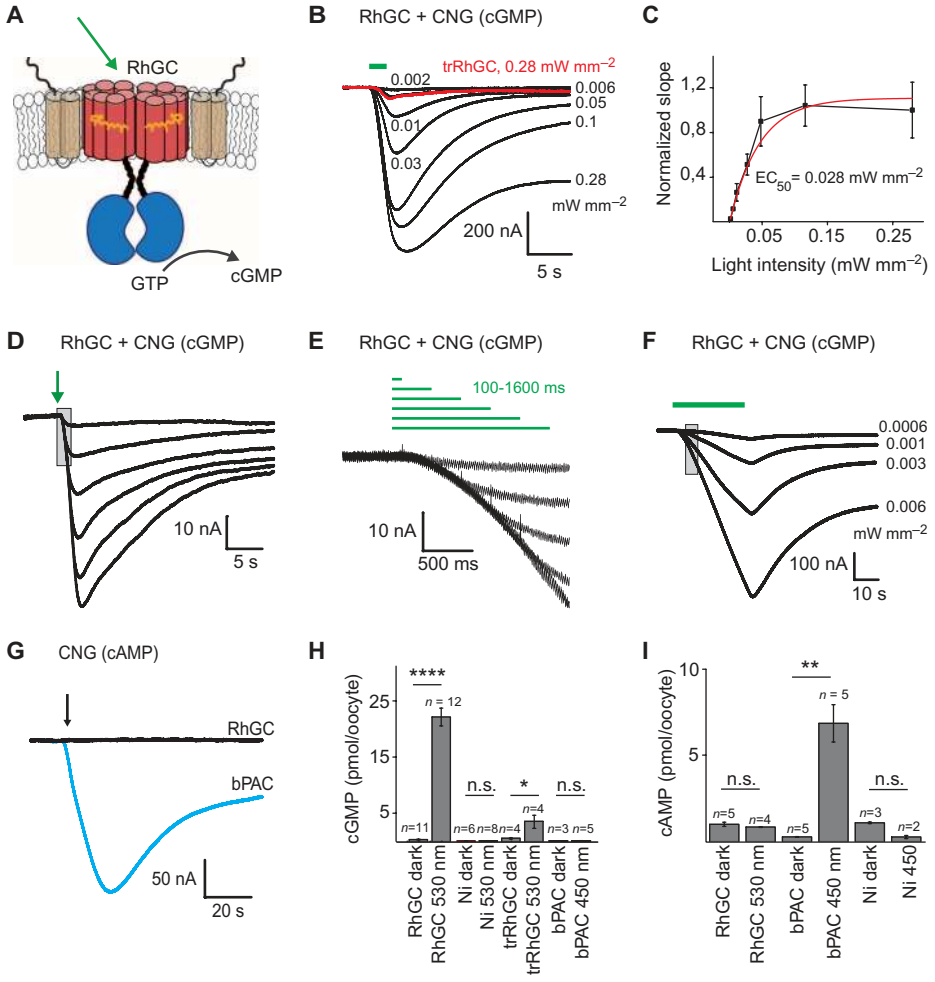

Fig. 1. Model of RhGC and its activity in *Xenopus* oocytes. (**A**) Model of dimeric RhGC with seven conserved transmembrane helices (red) and two additional membrane-spanning helices (beige). (**B**) Oocytes were injected with cRNA for the cGMP-sensitive CNG-A2 and cRNA for either RhGC (black traces) or RhGC with a truncated N terminus (trRhGC; red trace). Cells were irradiated for 2 s with 560-nm light at intensities of 0.002 to 0.28 mW mm^{-2} (half-bandwidth, 60 nm), and inward currents were measured as described in Materials and Methods. Current slopes were determined between 20 and 80% of the linear increase in signal. (**C**) Normalized slopes derived from six different cells were plotted against light intensity and fitted monoexponentially. The half-maximal light intensity (EC_{50}) value was determined at 0.028 mW mm^{-2} (correlation, R^2 = 0.992). (**D** to **F**) Oocytes were injected with cRNA for RhGC and cGMP-sensitive CNG. (D) Cells were stimulated with 530-nm light flashes of 0.006 mW mm^{-2} intensity for durations of 0.1, 0.4, 0.7, 1.0, 1.3, and 1.6 s (−20 mV holding potential), and inward currents were measured. (E) Enlargement of the gray region in (D) shows the initial current rise at different durations of stimulation. (F) Injected oocytes were stimulated for 30 s with 530-nm light at different intensities (−20 mV holding potential), and currents were measured. (**G**) Photocurrents of oocytes coexpressing the cyclic adenosine monophosphate (cAMP)–sensitive CNG-A2 (C460W/E583M) variant channel with RhGC (black trace) or *Beggiatoa* photoactivated adenylyl cyclase (bPAC) (blue trace). Traces in (B) to (G) are representative of at least five oocytes. (**H** and **I**) Oocytes were injected with cRNAs for the indicated constructs. Five days later, single oocytes were kept in the dark or were illuminated for 5 min with 530-nm light (0.010 mW mm^{-2}) or 450-nm light (0.015 mW mm^{-2}). The amounts of cGMP (H) and cAMP (I) were determined by ELISA. The amount of cGMP in RhGC-injected cells was statistically significantly increased after light exposure ($P < 0.0001$, Kruskal-Wallis), as was the amount of cAMP after blue light illumination of bPAC-injected oocytes. Data are means ± SEM. The number of experiments performed is shown. At least three oocytes were analyzed per experiment. *$P < 0.05$, **$P < 0.01$, ****$P < 0.001$, Mann-Whitney comparison. n.s., not significant.

Next, we determined the cGMP concentrations in oocytes with a competitive immunoassay (Fig. 1H). Five days after the oocytes were injected with cRNA, 0.2 ± 0.04 pmol of cGMP was extracted from cells that were kept in the dark for at least 1 hour (dark-adapted cells). The value was slightly greater than the amount of cGMP that was extracted from uninjected cells (0.1 ± 0.01 pmol per oocyte); however, 5-min illumination of the RhGC-expressing cells with green light (530 nm, 0.01 mW mm^{-2}) increased the intracellular cGMP concentration ~100-fold to 22.1 ± 1.6 pmol per oocyte (Fig. 1H). The actual dynamic range of RhGC might be even larger, because the intracellular cGMP concentration depends on the activities of both cyclases and endogenous esterases. Expression of trRhGC (see fig. S1) in cells resulted in a ~20-fold reduction in photocurrent amplitudes compared to those cells expressing full-length RhGC (Fig. 1B, red trace) and a ~6-fold reduction in cGMP abundance (Fig. 1H), which suggests that the N terminus plays a role in cyclase function, cyclase activation, or the folding and trafficking of RhGC to the plasma membrane. The intracellular concentration of cAMP in RhGC-expressing cells was above basal amounts but was not affected by illumination (Fig. 1I), further supporting our finding of the high GTP selectivity of RhGC in electrical measurement experiments (Fig. 1, B to G). Conversely, the abundance of cAMP increased in bPAC-expressing cells upon their illumination with blue light (470 nm, 0.015 mW mm^{-2}).

Activation of RhGC in CHO cells

To analyze RhGC activity in mammalian cells, we stably expressed mCherry-tagged RhGC in a preexisting CHO K1 cell line already expressing a cGMP-sensitive bovine CNG-A2 channel ($K_{1/2}^{cAMP}$ = 14 μM, $K_{1/2}^{cGMP}$ = 0.7 μM) (*8*). Intracellular Ca^{2+} concentrations, as reported by Fluo-4 or Fura-2 fluorescence, increased substantially upon repetitive flashing of the cells with 485-nm light from the Xenon lamp of the plate reader in a light dose–dependent manner (Fig. 2A). The light-induced increase in the intracellular concentration of cGMP ($[cGMP]_i$) was fully reversible without a large decrease upon repetitive illumination (adaptation) (Fig. 2B).

Characterization of recombinant RhGC

Alignment of the sequence of the rhodopsin fragment of *B. emersonii* RhGC with that of

other rhodopsins (fig. S1) and a three-dimensional (3D) model based on the structure of the sensory rhodopsin NpSRII (fig. S2) revealed that the rhodopsin fragment of *B. emersonii* is a typical microbial rhodopsin with a retinal-binding pocket for all-trans-retinal and a conserved active site. To assess the spectral properties of RhGC, we purified the recombinant rhodopsin fragment (amino acid residues 1 to 396; fig. S1) from the methylotrophic yeast *Pichia pastoris*. The full-length RhGC could not be purified in sufficient amounts. The dark-adapted rhodopsin fragment (termed D525) showed a typical unstructured rhodopsin spectrum with a maximum absorption at 525 nm (Fig. 3A). Bright green illumination (530 nm) converted D525 into a species with a deprotonated chromophore that absorbed maximally at 380 nm (P380) (Fig. 3A), which we considered to be the main intermediate of the cyclic reaction pathway (photocycle) and most likely the signaling state. After short illumination (5 s), P380 fully converted back to D525, whereas after a long illumination (5 min), a substantial fraction of the rhodopsin fragment was not reconverted to the dark state probably because of the reduced stability of the photoproducts in detergent (Fig. 3A). Stimulation with a 10-ns laser flash unveiled the reversible dynamics of the photocycle. P380 was formed with a time constant $\tau = 8$ ms after flash and reverted with $\tau = 93$ ms at 22°C and pH 8 (Fig. 3B). However, the depletion and recovery kinetics of the dark state monitored at 505 and 550 nm were both biexponential, which suggested the existence of additional photoproducts before and after formation of P380 (Fig. 3B and Table 1). To address this question, we recorded a series of spectra between 350 and 650 nm after laser stimulation of the recombinant rhodopsin (Fig. 3C). Before the formation of P380, the spectra revealed an early red-shifted photoproduct, P580, which converted into P380 within 8 ms. *Pichia* membranes containing full-length RhGC were used for further characterization of the cyclase activity. We found that in green light, RhGC exhibited a very stable activity with an initial velocity of 1 nmol cGMP per second per nanomole of RhGC at 1 mM GTP-RhGC, whereas in darkness, RhGC was totally inactive (at least 10,000-fold less active compared to RhGC in the light) (Fig. 3D; see Materials and Methods for the calculation).

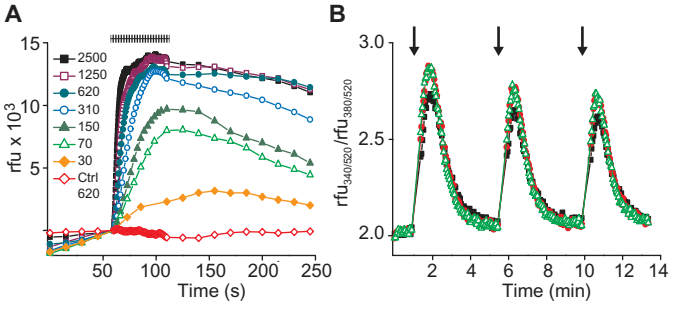

Fig. 2. Activity of RhGC stably expressed in CHO K1 cells. (A) CHO K1 cells stably coexpressing RhGC-mCherry and the cGMP-sensitive channel CNG-A2 were stimulated for 50 s (black, dashed bar) by 30 to 2500 flashes of 485-nm light of 1.3 W mm^{-2} as indicated, and Ca^{2+} signals of cells in 96-well microplates were monitored with Fluo-4. CHO K1 cells expressing CNG-A2 alone were used as a control (red) and were stimulated with 620 flashes. Data are means of triplicate wells and are representative of at least two independent experiments. (B) CHO K1 cells stably coexpressing RhGC-mCherry and the cGMP-sensitive CNG channel CNG-A2 were subjected to repetitive stimulation (black arrows, white light; 15 s, 1.3 μW mm^{-2}), and the recovery of the RhGC activity was monitored by Fura-2 fluorescence. Data are means of triplicate wells and are representative of at least two independent experiments. rfu, relative fluorescence units.

Expression of RhGC in hippocampal neurons

As proof of concept for optogenetic applications, we tested the function of RhGC in rat hippocampal CA1 neurons (Fig. 4A). Bright green light activated endogenous currents of less than −20 pA in neurons expressing RhGC (Fig. 4B; −11.7 ± 2.8 pA, $n = 3$ neurons). When the cGMP-sensitive channel CNG-A2 was coexpressed with RhGC, large inward currents were evoked by green light (Fig. 4B). Therefore, light-activated RhGC increased neuronal cGMP concentrations and activated CNG-A2 in CA1 neurons. The almost complete absence of currents in neurons expressing RhGC alone suggests that CA1 neurons have almost no endogenous cGMP-activated channels and that RhGC does not itself have substantial ion channel or ion-pumping activity. The action spectrum showed a peak at ~530 nm (Fig. 4, C and D), which is consistent with the absorption spectrum of

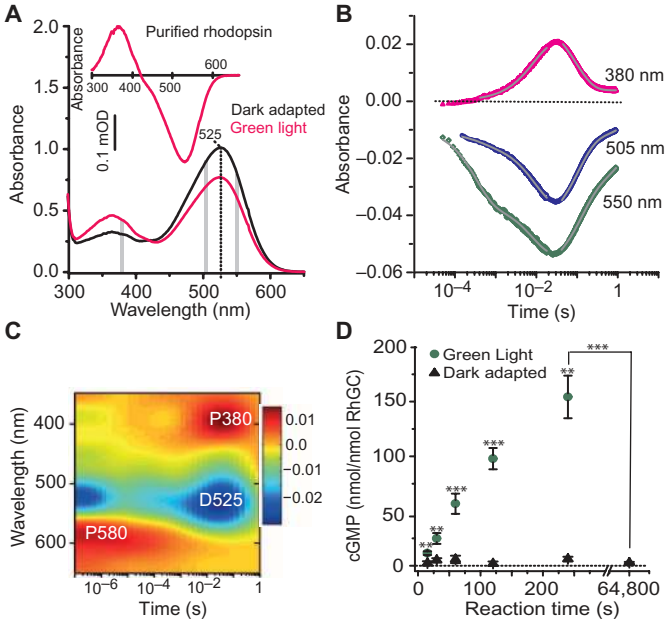

Fig. 3. Photochemical characterization of RhGC and analysis of cGMP production. (A) Absorption spectrum of the recombinant rhodopsin fragment in detergent at pH 8 before (black) and after (magenta) a 1-min illumination with 505-nm light (0.07 mW mm^{-2}). Gray bars indicate which wavelengths were used to monitor photocycle intermediates. Inset: Difference spectrum of "illuminated" minus "dark" spectra reveals bleaching of the dark-adapted state at 525 nm and its conversion into P380. mOD, milli-optical density. (B) Transient absorption changes recorded at 380, 505, and 550 nm after application of a 10-ns, 525-nm laser flash [see also the gray bars in (A)]. (C) Reconstruction of the time-resolved absorbance changes of the rhodopsin fragment between 350 and 650 nm at pH 8 from 10^{-7} to 1 s after excitation with a 10-ns flash of 525-nm light. Gradual absorbance changes are color-coded, as indicated by the sidebar. The analysis is based on the most prevalent components as obtained by singular value decomposition. (D) Plasma membranes containing RhGC were prepared from *P. pastoris*, and 10 μg of aliquots was incubated with 1 mM GTP and were either exposed to green light (circles) or incubated in the dark (triangles). Aliquots were taken from a reaction mixture after 10, 30, 60, 120, or 240 s and after 18 hours and were analyzed for cGMP content by HPLC. Data are means of three experiments. Illuminated values were compared to dark values (**$P < 0.01$, ***$P < 0.001$). Integration of peak areas yielded initial reaction velocities.

Table 1. Kinetic constants for the rise and decay of rhodopsin fragment photocycle intermediates.

Detection wavelength (nm)	Kinetic constants
380	τ_{rise} = 8 ± 0.6 ms τ_{decay} = 93 ± 1 ms
505	τ_{rise1} = 0.38 ± 0.15 ms τ_{rise2} = 9.2 ± 2.1 ms τ_{decay1} = 104 ± 1 ms τ_{decay2} = 20 ± 9.8 s
550	τ_{rise1} = 0.32 ± 0.19 ms τ_{rise2} = 7.8 ± 0.59 ms τ_{decay1} = 120 ± 2 ms τ_{decay2} = 1.9 ± 0.6 s

dark-adapted RhGC (Fig. 3A). Light pulses applied every 5 s yielded photocurrents of very reproducible amplitude (Fig. 4E).

The dendritic morphology of CA1 neurons expressing RhGC, CNG-A2, and the far-red fluorescent protein mKate2 (Fig. 5A) was indistinguishable from that of CA1 cells expressing mKate2 alone. Transfected neurons showed normal resting membrane potential and spiking behavior in response to depolarizing current steps (Fig. 5, B and C). Thus, RhGC expression was well tolerated in neurons, which was suggestive of good folding of the RhGC protein, as well as little or no dark activity. The amplitude of each photocurrent depended on light intensity (Fig. 5D). The light sensitivity of RhGC-expressing cells (Fig. 5E) was comparable to that of channelrhodopsin-2–expressing cells (EC_{50} ≈ 1.1 mW mm^{-2}) (*9*). Varying the duration of saturating light pulses (at an intensity of 19.2 mW mm^{-2}) resulted in photocurrents with uniform slopes but graded amplitudes (Fig. 5F). The time to onset of the currents was 120 ± 30 ms (Fig. 5F; median = 85 ms). Together, these results suggest that $[cGMP]_i$ can be optogenetically controlled in a quantitative, reversible, and reproducible manner in mammalian neurons.

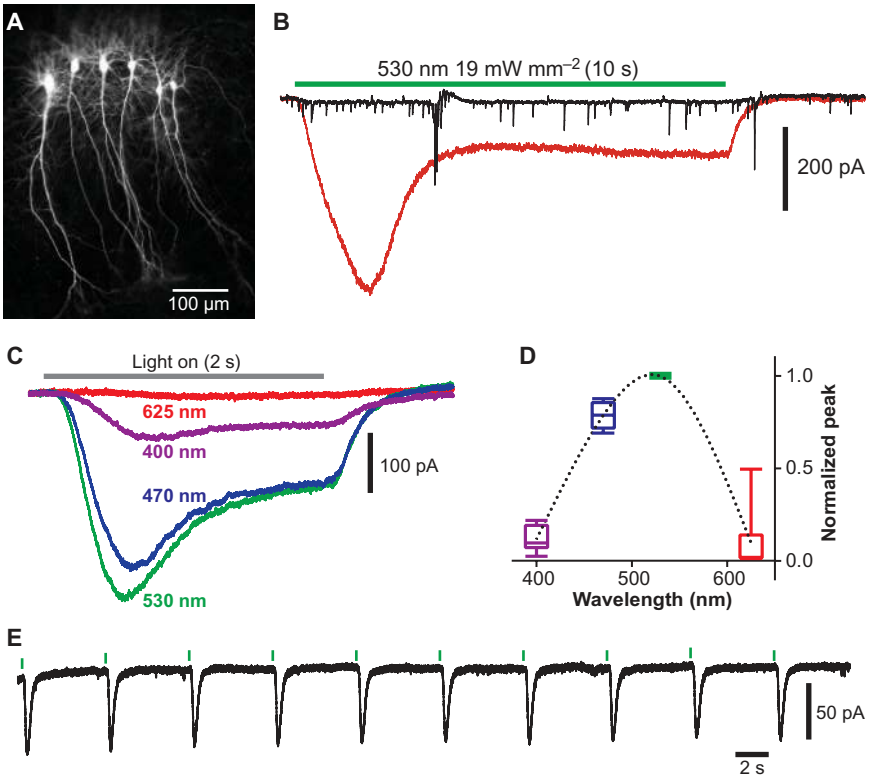

Fig. 4. Light-induced cGMP signaling in neurons expressing RhGC. (**A**) Fluorescence image of CA1 neurons in a hippocampal slice culture 10 days after electroporation with plasmids encoding RhGC and mKate2. (**B**) CA1 hippocampal neurons expressing RhGC alone (black trace, representative of three neurons) or RhGC and the cGMP-selective channel CNG-A2 (red trace) were illuminated with green light (530 nm, 19.2 mW mm^{-2}, 10 s), and inward currents were measured with whole-cell, patch-clamp recordings at –65 mV. Fast deflections in cells expressing RhGC alone were spontaneous synaptic events that were not blocked in this example. (**C** and **D**) Determination of the wavelength dependence in neurons. (C) Sample photocurrents showing the dependences on the wavelength of submaximal light pulses (1 mW mm^{-2}, 2 s). (D) Summary of the activation spectra determined from six neurons for each wavelength of light. Boxes are medians with 25 to 75 percentiles; whiskers show minimum and maximum values. (**E**) Photocurrents evoked by brief light pulses (green ticks, 530 nm, 1 mW mm^{-2}, 100 ms) were fully reversible and reproducible at a frequency of 0.2 Hz. Data are representative of three neurons.

DISCUSSION

We validated the hypothesis that the microbial rhodopsin of the fungus *B. emersonii* functions as a directly light-activated GC. To sense light, this fungus has developed a distinct light sensor that combines the function of a light-absorbing rhodopsin and a highly specific cyclase into a single molecule, without the need for an intermediary transducer module. This strategy is different from all other behavioral photoreceptor transduction cascades described thus far.

By expressing and functionally characterizing RhGC in three different heterologous systems, we showed that it has the potential to become a widely used optogenetic tool for the exploration of cGMP signaling. cGMP is an important signaling molecule in many eukaryotes, including mammals. Vision and olfaction critically depend on cGMP, as do such processes as muscle contraction, homeostasis, and cardiovascular function (*10*). Optical control of the cGMP system would be very desirable, although a photoactivatable GC (BlgC) engineered from bPAC has been described (*11*); however, BlgC has substantial dark activity and also has ~10% residual adenylyl cyclase (AC) activity in vitro. In contrast, RhGC did not have detectable AC activity in oocytes, indicating that it has a high selectivity for GTP. Furthermore, our in vitro assay with recombinant RhGC showed that the enzyme had an undetectable activity in darkness. Another advantage of rhodopsins over flavin-based photoreceptor domains is the possibility of tuning the absorption wavelength and kinetic properties to suit the experimental demands (*12*, *13*). Similar to channelrhodopsins, RhGC

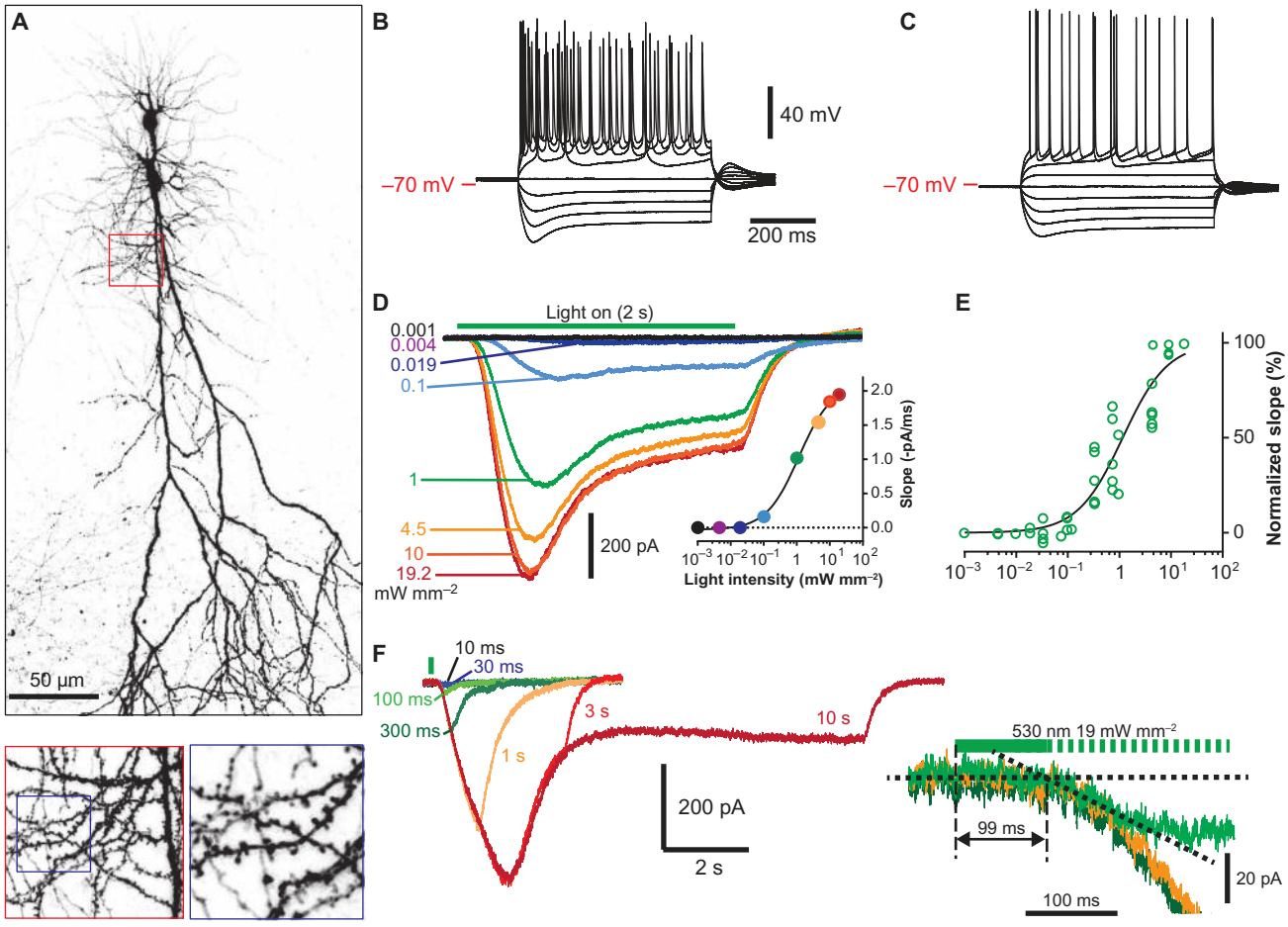

Fig. 5. RhGC enables light dose–dependent control of cGMP production in neurons. (**A**) A two-photon maximum intensity projection of CA1 neurons 7 days after electroporation with plasmids encoding RhGC, the cGMP-sensitive channel CNG-A2, and mKate2. Red box, 40 × 40 µm; blue box, 18 × 18 µm. (**B** and **C**) The membrane response of two CA1 neurons expressing RhGC and CNG-A2 to somatic current injections (−400 to 400 pA). (**D**) Whole-cell photocurrents measured at −75 mV in response to light of increasing intensity (530 nm, 2 s). Inset shows dose-response relationship for this example, curve generated with a logistic equation. (**E**) Normalized slopes versus light intensities for seven neurons for each condition were fitted with a logistic equation. Hill slope = 0.994 (95% confidence interval, 0.758 to 1.23); EC_{50} = 1.57 mW mm^{-2} (95% confidence interval, 0.88 to 1.52); R^2 = 0.91. (**F**) Photocurrents measured by whole-cell voltage-clamp recordings at −75 mV in response to light pulses of increasing duration (530 nm, 19.2 mW mm^{-2}). Inset shows close-up of the 100-ms to 1-s traces to illustrate how time to onset of response was measured. Data are representative of seven cells. Traces in (B), (D), and Fig. 4C are from the same cell. Traces in (C) and Fig. 4E are from the same cell.

can be activated repetitively without obvious bleaching effects, which is an important feature for reproducible optical stimulation.

MATERIALS AND METHODS

Molecular biology

A full-length, human codon–optimized DNA sequence encoding RhGC of *B. emersonii* (accession no. KP731361, a humanized version of KF309499) was purchased from GenScript, subcloned into the Bam HI and Hind III sites of pGEM (Promega), and used for cRNA synthesis. To express RhGC in CHO K1 cells, the 3′ end of the complementary DNA (cDNA) encoding RhGC was fused to the cDNA encoding mCherry and subcloned into the Xba I and Bam HI sites of the pcDNA6/V5-His A plasmid (Life Technologies). The resulting construct was designated as pc6RhGC-mCherry.

Characterization of RhGC in *Xenopus* oocytes

Oocytes were prepared from female *X. laevis* as described previously (*14*). Single oocytes were injected with combinations of different cRNAs and incubated in Ringer's solution supplemented with 1 µM all-trans-retinal (Sigma). RhGC was coexpressed with the cGMP-sensitive CNG-A2 channel [rat olfactory, gb: 6978671 or the cAMP-sensitive version (C460W/E583M)]. Therefore, oocytes were coinjected with 2.5 ng of cRNA for RhGC or trRhGC and 5 ng of cRNA for the cGMP-sensitive CNG (Fig. 1, B and C), whereas oocytes were coinjected with 5 ng of each cRNA for the experiments depicted in Fig. 1 (D to F). For the experiments shown in Fig. 1G, the oocytes were injected with 5 ng of cRNA for RhGC together with 5 ng of cRNA for the cAMP-sensitive CNG channel. Control cells were injected with 100 pg of cRNA for bPAC and 20 ng of cRNA for the cAMP-sensitive CNG variant (Fig. 1G). Photocurrents were measured in oocytes 3 to 5 days after they were injected with cRNA. For two-electrode,

voltage-clamp measurements and data acquisition, we used a TURBO TEC-03X amplifier (NPI Electronic) and pCLAMP 9.0 software (Molecular Devices). Microelectrodes were fabricated from borosilicate glass capillaries (1.50 mm outer diameter and 1.17 mm inner diameter) with a micropipette puller (model no. P-97, Sutter Instrument) and filled with 3 M KCl. Microelectrode resistance was 0.5 to 1.5 megohms. The actinic light of an XBO 75W Xenon lamp (Osram) was controlled by an LS3 shutter (Vincent Associates UNIBLITZ) and filtered by a 560-nm wideband filter (K55 Balzers, half-bandwidth, 60 nm) or a 530-nm filter (20BPF10-530 8C057, Newport; half-bandwidth, 9 nm). Light intensity was decreased with the help of neutral density filters. The composition of the extracellular buffer was 96 mM NaCl, 5 mM KCl, 0.1 mM $CaCl_2$, 1 mM $MgCl_2$, 5 mM Hepes (pH 7.5). Oocytes were voltage-clamped at −20 or −40 mV. The functionality of the cAMP-sensitive CNG channel (C460W/E583M) was shown through coexpression with bPAC and 3-s illumination with 450-nm light of 0.03 mW mm^{-2}. Data were analyzed with Stimfit 0.13 (*15*) and Clampfit 10.4 software (Molecular Devices LLC).

Enzyme-linked immunosorbent assays

Five days after they were injected with cRNA [10 ng for RhGC or trRhGC, 100 pg for bPAC (Fig. 1H), or 1 ng for bPAC (Fig. 1I); control cells: uninjected], three of the respective oocytes were pooled and either kept in the dark or illuminated with 522-nm (0.010 mW mm^{-2}) or 470-nm (0.015 mW mm^{-2}) light of a light-emitting diode (LED) array (Adafruit NeoPixel NeoMatrix 8×8 - 64 RGB). Oocytes were disrupted in 300 µl of 0.1 M HCl by vigorous pipetting. Cell debris and protein (>10 kD) were removed through three successive centrifugation steps at 4°C: first, 7 min at 16,000*g*; second, 7 min at 15,000*g* with a 0.22-µm Spin-X cellulose acetate membrane centrifugal filter (Corning Costar); and third, 30 min at 14,000*g* with an Ultra-0.5 Centrifugal Filter with Ultracel-10 membrane (Amicon). The amount of cGMP in the purified lysate was determined with a direct cGMP enzyme-linked immunosorbent assay (ELISA) kit (Enzo Life Sciences), according to the manufacturer's instructions. To calculate cGMP abundance, an oocyte volume of 1 µl was assumed. Mean values and SEs of between 2 and 10 individual samples derived from three different frogs are shown in Fig. 1H. To analyze cAMP abundance (Fig. 1I), illumination and lysate purification were performed as described earlier, except that a direct cAMP ELISA kit (Enzo Life Sciences) was used.

Generation of stable cell lines

CHO K1 cells stably expressing a CNG-A2 channel–based cGMP sensor (*8*) were electroporated with pc6RhCG-mCherry with the Neon 100 Kit (Invitrogen) and a MicroPorator (Digital Bio) according to the manufacturer's protocol (3× 1650-mV pulses with a 10-ms pulse width). Cells were transferred into complete medium composed of F12 plus GlutaMAX (Invitrogen) and 10% fetal bovine serum (Biochrom). To select monoclonal cells stably expressing RhGC, the antibiotics G418 (400 µg/ml; Invitrogen) and blasticidin (50 µg/µl; Invitrogen) were added to the cell culture medium 24 hours after the electroporation was performed. Monoclonal cell lines were identified by their expression of mCherry as determined by fluorescence microscopy.

Fluorescence-based RhGC assays

The activity of heterologously expressed RhGC in CHO K1 cells was monitored with a cGMP-sensitive CNG-A2 channel and Fluo-4 or Fura-2 (Life Technologies). Assays were performed in 96-well plates (Greiner) with a FLUOstar Omega reader (BMG Labtech) at 29°C. Ratiometric Fura-2 measurements were performed by excitation at 340 and 380 nm and detection of emission at 510 nm. For Fluo-4 measurements, 485- and 520-nm filters were used for excitation and emission, respectively. All bandpass filters had a half-bandwidth of 10 nm. RhGC was stimulated by 485-nm flashes of the Xenon lamp in the plate reader or by an external light source (530 nm, 0.0013 mW mm^{-2}). Stimuli of different intensities were achieved by varying the numbers of flashes. Data analysis was performed with the reader software MARS (BMG Labtech) and Origin software (OriginLab Corp.).

Spectroscopic analysis of recombinant proteins

For heterologous expression of full-length RhGC and the rhodopsin domain (corresponding to amino acid residues 1 to 396) in *P. pastoris* cells (strain 1168H, Invitrogen), DNA sequences were subcloned into the pPICZ plasmid (Invitrogen), which contains a C-terminal polyhistidine tag (6×His), at the Eco RI and Not I restriction sites. Cell transformations, cell culture, and protein purifications were performed as described previously (*16*). After protein expression was induced for 24 hours, cells were harvested and gently lysed with a high-pressure homogenizer (AVESTIN). The membrane fraction containing the rhodopsin fragment was collected, homogenized, and solubilized in 1% (w/v) dodecylmaltoside (DDM). After binding of the rhodopsin fragment protein to Ni–nitrilotriacetic acid resin (5 ml of His trap crude column, GE Healthcare) and washing of the column with 10 column volumes of 50 mM imidazole, the rhodopsin fragment was eluted with 500 mM imidazole. Fractions that contained the protein were pooled, desalted (through a HiPrep 26/10 Desalting column, GE Healthcare), and concentrated with an Amicon Ultra 100 kD (Millipore) in tris buffer [50 mM tris (pH 8.0), 100 mM NaCl, 0.03% DDM, 0.1 mM phenylmethylsulfonyl fluoride] to an optical density of 1 at 525 nm. Spectra were recorded in a Cary 50 Bio spectrophotometer (Varian Inc.) at 20°C at a spectral resolution of 1.6 nm. Light spectra were recorded after 1 min of illumination with a green LED (505 nm, 0.07 mW mm^{-2}). Transient spectroscopy was performed on an LKS.60 flash photolysis system (Applied Photophysics Ltd.) at 22°C. Excitation pulses of 10 ns (at 525 nm) were provided by a tunable Rainbow OPO/Nd:YAG laser system. Laser energy was adjusted to 6 mJ per shot. The instrument used a Xenon lamp (150 W) as a monitoring light source, which was pulsed during short-time experiments. Data analysis was performed with MATLAB 7.01 software (The MathWorks). Singular value decomposition of representative data sets was performed to identify statistically significant components that were used for reconstruction of the 3D spectra. Time constants were obtained by fitting exponential functions to the data.

HPLC assay of cGMP formation

Membranes of RhGC-expressing *P. pastoris* were prepared as described earlier with tris buffer containing 5 mM $MnCl_2$ and 0.1 mM GTP to stabilize the protein. After centrifugation, membranes were washed in tris buffer without GTP. Catalytic activity was measured at 25°C in 100 µl of Ringer's solution with 1.0 to 1.5 mg of total membrane protein. Samples were kept in the dark or were illuminated with 522-nm light with an intensity of 0.01 mW mm^{-2} (LED array, Adafruit NeoPixel NeoMatrix 8×8 - 64 RGB). Reactions were started by adding 1 mM GTP. Aliquots were taken at different time points and were immediately frozen in liquid nitrogen. Two hundred microliters of 0.1 N HCl was added, and thawed samples were centrifuged and filtered (0.2-µm pore size, Chromafil; Macherey-Nagel) to remove the membrane and denatured protein. Nucleotides were separated by high-performance liquid chromatography (HPLC) with a C18 reversed-phase column (Supelco, Sigma-Aldrich) and 100 mM potassium phosphate (pH 5.9), 4 mM tetrabutylammonium iodide, and 10% (v/v) methanol as eluent. Nucleotides were monitored at 253 nm. Data were analyzed with

Origin software (OriginLab Corp.). Peak areas of GTP and cGMP were assigned and integrated by comparing retention times with the corresponding standard compounds. Since cGMP values in the dark were at detection threshold, we took an additional very late time point (18 hours) to increase the chance of detecting any accumulated product. To calculate the light-induced increase in cyclase activity, the light rate ($[cGMP]_{240s}$ divided by illumination time) was divided by the dark rate ($[cGMP]_{64800s}$ divided by incubation time). The amount of cGMP increased with light exposure ($P < 0.02$, Spearman's correlation = 1) but did not change in the dark ($P = 0.7$, Spearman's correlation = 0.26). The amount of RhGC ($M = 69{,}000$ daltons) was determined by calculating the amount from a Coomassie-stained SDS–polyacrylamide gel electrophoresis gel and comparing it to a known amount of a reference protein. A direct absorption measurement of purified, full-length RhGC was not possible because in our hands, the functional full-length protein could not be solubilized from the membrane.

Electrophysiology of hippocampal neurons

Hippocampal slice cultures from female Wistar rats were prepared on postnatal day 5 or 6 as described previously (*17*). No antibiotics were used in the preparation or culture medium. The following plasmids were prepared with the neuron-specific promoter synapsin-1 (syn): pAAV-syn-beRHGC-2A-tdimer2 (RhGC), rat CNG-A2 (PCI-syn-CNGA2), and PCI-syn-mKate2N. The RhGC and CNG-A2 plasmids were diluted to 25 ng/μl, whereas the mKate2 plasmid was diluted to 50 ng/μl in a K-gluconate–based pipette solution consisting of 135 mM potassium gluconate, 4 mM $MgCl_2$, 4 mM Na_2–adenosine triphosphate, 0.4 mM Na-GTP, 10 mM sodium phosphocreatine, 3 mM ascorbate, and 10 mM Hepes (pH 7.2, 295 mosmol, electroporation pipette resistance ~14 megohms). Slices were submerged in solution containing 145 mM NaCl, 10 mM Hepes, 25 mM D-glucose, 2.5 mM KCl, 1 mM $MgCl_2$, and 2 mM $CaCl_2$ (pH 7.4, ~311 mosmol). An Axoporator 800A (Molecular Devices) was used to deliver the DNA to loosely patched neurons [50 pulses (−12 mV, 0.5 ms) at 50 Hz] (*18*). Four to 10 days later, whole-cell patch-clamp recordings were established at 30°C in artificial cerebrospinal fluid containing 127 mM NaCl, 2.5 mM KCl, 2 mM $CaCl_2$, 1 mM $MgCl_2$, 25 mM $NaHCO_3$, 1.25 mM NaH_2PO_4, and 25 mM D-glucose (pH 7.4, ~308 mosmol, saturated with 95% O_2/5% CO_2). In most experiments, 10 μM NBQX, 10 μM CPPene, and 100 μM picrotoxin were added to block fast excitatory and inhibitory synaptic transmission. Recording pipettes (3 to 6 megohms) were filled with the same intracellular solution that was used for electroporation (without the DNA). Cells were voltage-clamped at −65 mV, and currents were recorded with an Axoclamp200B (Molecular Devices) and Ephus software (*19*). Series resistance was less than 20 megohms. For photostimulation of RhGC, a four-color LED light source (Mightex) was coupled to the camera port of a BX61WI microscope (Olympus) through a multimode fiber (1.0 mm) and collimator (Thorlabs). Radiant power was measured with a silicon photodiode (LaserCheck) in the specimen plane (objective lens used, Plan-Apochromat 40× 1.0 numerical aperture, Zeiss) and divided by the illuminated field (0.244 mm^2). To determine the action spectra, the illumination intensity from the four-color LEDs was set to match as closely as possible, and the currents were divided by the actual intensity to correct for small variations between LEDs before normalization. Analysis of the currents was performed with MATLAB, whereas graphs and curve-fitting were generated with GraphPad Prism 6.0.

Data analysis and statistics

All data are reported as means ± SEM and are derived from at least three independent biological experiments, unless otherwise stated in the figure legends or text. Statistical analyses and curve-fitting were performed with GraphPad Prism 6.0 or OriginPro 8G software. Nonparametric tests were preferentially used. To compare the amounts of cGMP and cAMP in illuminated cells with those in cells kept in the dark (Fig. 1, H and I), a Kruskal-Wallis test was performed, which was followed by Mann-Whitney pairwise comparisons. To compare the amounts of cGMP formed in dark-adapted and illuminated RhGC-containing membranes, unpaired *t* tests with a Holm-Sidak correction for multiple comparisons were applied after determination of the Spearman correlation coefficient (Fig. 3D). $P < 0.05$ was considered to be statistically significant.

SUPPLEMENTARY MATERIALS

www.sciencesignaling.org/cgi/content/full/8/389/rs8/DC1
Fig. S1. Sequence alignment of the rhodopsin domain of RhGC from different species.
Fig. S2. 3D model of the rhodopsin active site of RhGC based on the structure of NpSRII.
References (*20*–*22*)

REFERENCES AND NOTES

1. O. P. Ernst, D. T. Lodowski, M. Elstner, P. Hegemann, L. S. Brown, H. Kandori, Microbial and animal rhodopsins: Structures, functions, and molecular mechanisms. *Chem. Rev.* **114**, 126–163 (2014).
2. P. M. Silverman, Regulation of guanylate cyclase activity during cytodifferentiation of *Blastocladiella emersonii*. *Biochem. Biophys. Res. Commun.* **70**, 381–388 (1976).
3. J. Saranak, K. W. Foster, Rhodopsin guides fungal phototaxis. *Nature* **387**, 465–466 (1997).
4. G. M. Avelar, R. I. Schumacher, P. A. Zaini, G. Leonard, T. A. Richards, S. L. Gomes, A rhodopsin-guanylyl cyclase gene fusion functions in visual perception in a fungus. *Curr. Biol.* **24**, 1234–1240 (2014).
5. K. H. Biswas, A. R. Shenoy, A. Dutta, S. S. Visweswariah, The evolution of guanylyl cyclases as multidomain proteins: Conserved features of kinase-cyclase domain fusions. *J. Mol. Evol.* **68**, 587–602 (2009).
6. T. C. Rich, T. E. Tse, J. G. Rohan, J. Schaack, J. W. Karpen, In vivo assessment of local phosphodiesterase activity using tailored cyclic nucleotide–gated channels as cAMP sensors. *J. Gen. Physiol.* **118**, 63–78 (2001).
7. M. Stierl, P. Stumpf, D. Udwari, R. Gueta, R. Hagedorn, A. Losi, W. Gärtner, L. Petereit, M. Efetova, M. Schwarzel, T. G. Oertner, G. Nagel, P. Hegemann, Light modulation of cellular cAMP by a small bacterial photoactivated adenylyl cyclase, bPAC, of the soil bacterium *Beggiatoa*. *J. Biol. Chem.* **286**, 1181–1188 (2011).
8. W. Altenhofen, J. Ludwig, E. Eismann, W. Kraus, W. Bönigk, U. B. Kaupp, Control of ligand specificity in cyclic nucleotide-gated channels from rod photoreceptors and olfactory epithelium. *Proc. Natl. Acad. Sci. U.S.A.* **88**, 9868–9872 (1991).
9. J. Y. Lin, M. Z. Lin, P. Steinbach, R. Y. Tsien, Characterization of engineered channelrhodopsin variants with improved properties and kinetics. *Biophys. J.* **96**, 1803–1814 (2009).
10. K. A. Lucas, G. M. Pitari, S. Kazerounian, I. Ruiz-Stewart, J. Park, S. Schulz, K. P. Chepenik, S. A. Waldman, Guanylyl cyclases and signaling by cyclic GMP. *Pharmacol. Rev.* **52**, 375–414 (2000).
11. M. H. Ryu, O. V. Moskvin, J. Siltberg-Liberles, M. Gomelsky, Natural and engineered photoactivated nucleotidyl cyclases for optogenetic applications. *J. Biol. Chem.* **285**, 41501–41508 (2010).
12. A. Berndt, O. Yizhar, L. A. Gunaydin, P. Hegemann, K. Deisseroth, Bi-stable neural state switches. *Nat. Neurosci.* **12**, 229–234 (2009).
13. C. Bamann, R. Gueta, S. Kleinlogel, G. Nagel, E. Bamberg, Structural guidance of the photocycle of channelrhodopsin-2 by an interhelical hydrogen bond. *Biochemistry* **49**, 267–278 (2010).
14. A. Vogt, J. Wietek, P. Hegemann, *Gloeobacter* rhodopsin, limitation of proton pumping at high electrochemical load. *Biophys. J.* **105**, 2055–2063 (2013).
15. S. J. Guzman, A. Schlögl, C. Schmidt-Hieber, Stimfit: Quantifying electrophysiological data with Python. *Front. Neuroinform.* **8**, 16 (2014).
16. C. Bamann, T. Kirsch, G. Nagel, E. Bamberg, Spectral characteristics of the photocycle of channelrhodopsin-2 and its implication for channel function. *J. Mol. Biol.* **375**, 686–694 (2008).
17. L. Stoppini, P. A. Buchs, D. Muller, A simple method for organotypic cultures of nervous tissue. *J. Neurosci. Methods* **37**, 173–182 (1991).
18. J. Rathenberg, T. Nevian, V. Witzemann, High-efficiency transfection of individual neurons using modified electrophysiology techniques. *J. Neurosci. Methods* **126**, 91–98 (2003).
19. B. A. Suter, T. O'Connor, V. Iyer, L. T. Petreanu, B. M. Hooks, T. Kiritani, K. Svoboda, G. M. Shepherd, Ephus: Multipurpose data acquisition software for neuroscience experiments. *Front. Neural Circuits* **4**, 100 (2010).

20. J. D. Thompson, D. G. Higgins, T. J. Gibson, CLUSTAL W: Improving the sensitivity of progressive multiple sequence alignment through sequence weighting, position-specific gap penalties and weight matrix choice. *Nucleic Acids Res.* **22**, 4673–4680 (1994).
21. C. Cole, J. D. Barber, G. J. Barton, The Jpred 3 secondary structure prediction server. *Nucleic Acids Res.* **36**, W197–W201 (2008).
22. M. Biasini, S. Bienert, A. Waterhouse, K. Arnold, G. Studer, T. Schmidt, F. Kiefer, T. G. Cassarino, M. Bertoni, L. Bordoli, T. Schwede, SWISS-MODEL: Modelling protein tertiary and quaternary structure using evolutionary information. *Nucleic Acids Res.* **42**, W252–W258 (2014).

Acknowledgments: We thank W. Bönigk, L. Geist, R. Hagedorn, J. Klotz, N. Liem, I. Ohmert, M. Reh, C. Schnick, and C. Wittig for excellent technical support. We are grateful to D. Wachten for stimulating discussion and critical reading of the manuscript. **Funding:** This work was supported by the German Research Foundation (Cluster of Excellence "Unifying Concepts in Catalysis" and SFB 1078 project B1 and B2 to P.H. and SPP1665 to P.H. and T.G.O.) and by the Belgian IWT (Optobrain to P.H.). **Author contributions:** U.S. performed all of the experiments with oocytes, including quantification of cGMP and cAMP; K.S. purified recombinant proteins and performed experiments with them; C.E.G. performed experiments with neurons; H.G.K. performed experiments in CHO K1 cells; R.F. analyzed sequences; P.H. and T.G.O. designed experiments; and U.S., K.S., C.G., T.O., and P.H. analyzed experiments and wrote the paper. **Competing interests:** The authors declare that they have no competing interests. **Data and materials availability:** All data and materials are freely available without the need for a materials transfer agreement, and plasmids will be available at Addgene.

Submitted 5 March 2015
Accepted 16 July 2015
Final Publication 11 August 2015
10.1126/scisignal.aab0611
Citation: U. Scheib, K. Stehfest, C. E. Gee, H. G. Körschen, R. Fudim, T. G. Oertner, P. Hegemann, The rhodopsin–guanylyl cyclase of the aquatic fungus *Blastocladiella emersonii* enables fast optical control of cGMP signaling. *Sci. Signal.* **8**, rs8 (2015).